PAPER

Check for updates

Solution-processed high efficiency OLED harnessing a thermally cross-linked hole-transporting layer and exciplex-forming emission layer†

Meng-Ju Tsai,[a] Wei-Lun Huang,[b] Li-Ming Chen, [ID] [a] Guo-Lun Ruan,[b] Dian Luo, [ID] [c] Zong-Liang Tseng*[b] and Ken-Tsung Wong [ID] *[ad]

A new dicarbazole-based donor, **BCz3Ph**, for exciplex formation was synthesized and characterized. The new green (PL λ_{max} = 527 nm) exciplex **BCz3Ph**:PO-T2T (2:1) blend with a photoluminescence quantum yield (PLQY) of 43% and thermally activated delayed fluorescence (TADF) character was utilized as the emitting layer (EML) of solution-processed OLED devices. To facilitate hole injection into the EML, a new cross-linkable monomer, **BCzC4Sy**, adopting a dicarbazole core linked to a styrene group by a butyl chain was designed to realize a solvent resistant hole-transporting layer (HTL) after thermal polymerization. The flexible butyl (C4) bridge accounts for a lower polymerization temperature as compared to that of the methyl (C1)-bridged counterpart, **BCzC1Sy**, resulting in the formation of amorphous films with better solvent resistance as well as smoother morphology. The choice of dicarbazole as the HTL core not only suppresses the HTL-to-EML energy barrier, but also prevents the emission color variation stemming from the possible exciplex emission at the HTL/EML interface. The best OLED device with EQE$_{max}$ = 9.2%, CE$_{max}$ = 27.94 cd A^{-1} and PE$_{max}$ = 28.7 lm W^{-1} was obtained with a thermally polymerized **BCzC4Sy** film as the HTL. The device achieved a maximum luminance up to 22 000 cd m^{-2} together with a very low efficiency roll-off, retaining 97% efficiency at 1000 cd m^{-2} (EQE$_{1000cd}$ = 8.9%). More significantly, a 2 × 2 cm^2 device fabricated by slot-die coating gave good color homogeneity and rather high brightness and promising efficiency (EQE 5.0%), manifesting the potential of employing a thermally cross-linkable HTM and exciplex-based EML to produce high efficiency solution-processed OLEDs.

Introduction

Organic light emitting diodes (OLEDs) have been utilized to develop new displays and further applied to lighting applications.[1,2] In recent years, OLEDs employing organic emitters with thermally activated delayed fluorescence (TADF) that can achieve 100% internal quantum efficiency (IQE) have attracted a great deal of attention.[3–5] The basic principle of TADF is to minimize the energy gap (ΔE_{ST}) between the singlet state and triplet state, which allows the triplet excitons to be up-converted to singlet excitons through a reverse intersystem crossing (RISC) process with the aid of environmental thermal energy, thereby increasing the efficiency of OLED devices. In order to achieve a small ΔE_{ST}, the molecule should possess an intramolecular charge transfer (CT) excited state with the highest occupied molecular orbital (HOMO) and the lowest unoccupied molecular orbital (LUMO) distributed on the donor (D) and acceptor (A), respectively. The manipulation of the electronic coupling between D and A as well as the spatial overlap of the HOMO and LUMO can be rationally achieved through sophisticated molecular design, yet is often challenging regarding syntheses.[6–9] Therefore, another approach that incorporates the exciplex-forming system formed by optical or electrical excitation of a physically blended D and A pair has emerged.[10a–e] Since the HOMO and LUMO of exciplex excitons are localized on D and A molecules, respectively, the exciplex-forming system possesses a small ΔE_{ST} and thus TADF properties. The efficient RISC of the exciplex-forming system makes it

[a] *Department of Chemistry, National Taiwan University, Taipei, 10617, Taiwan. E-mail: kenwong@ntu.edu.tw*

[b] *Department of Electronic Engineering, Ming Chi University of Technology, New Taipei City 243303, Taiwan. E-mail: zltseng@mail.mcut.edu.tw*

[c] *College of Photonics, National Yang Ming Chiao Tung University, Tainan, 71150, Taiwan*

[d] *Institute of Atomic and Molecular Science, Academia Sinica, Taipei, 10617, Taiwan*

† Electronic supplementary information (ESI) available. See DOI: https://doi.org/10.1039/d2tc04638e

suitable for developing highly efficient OLED devices.[11–16] In addition, the D:A blends render the feasibility of preparing smooth films by solution processes given the stronger intermolecular interactions between D and A molecules, which might promote the efficiency of solution-processed exciplex-based OLEDs.[17] For example, Tseng and coworkers demonstrated the use of a TAPC:PO-T2T blend as the emitting layer (EML) with efficient green exciplex emission to fabricate a solution-processed device with EQE$_{max}$ of 7.1%.[18] Though solution-processed technologies for OLEDs are still under development, this promising method presents potential benefits over the mainstream physical vapor deposition, such as the exclusion of expensive vacuum equipment, effective material utilization efficiency, and scalable and uniform large-area film production on flexible substrates.[19] Typically, solution processes involve the coating of functional material solutions onto (indium tin oxide) ITO-treated substrates, followed by drying the layer to obtain films. For instance, water-soluble PEDOT:PSS is most commonly used as the hole injection layer (HIL), given its non-miscibility with organic solvents, which can then be followed by continuous deposition of multilayer stacks. It is crucial to use tailor-made functional materials for the solution process, where the small molecule materials used must present good solubility to facilitate the coating process and film formation.[20] Nevertheless, excessive solubility brings about the erosion of formerly deposited layers, which would give rise to uneven thickness or even pinholes in the films, leading to poor device efficiencies. Specifically, the hole-transporting layer (HTL) is deemed the most requisite layer to improve the anti-solvent property. To tackle this issue, several teams have designed small molecules with special functional groups to enhance the solubility for film fabrication, and are further polymerized with self-assembly,[21] photochemical reactions,[22] electrochemical reactions[23,24] or cross-linking[25,26] to produce polymers with strong resistance towards solvent erosion and intermixing with the other layers. Among cross-linking methods, photo cross-linking can be carried out at low temperatures and requires a short amount of time with the aid of initiators. However, the addition of initiators may also cause side reactions to occur, producing undesired impurities and thus affecting the efficiency of OLED devices. In contrast, despite the fact that thermal cross-linking requires higher temperatures, the absence of initiators would lead to fewer side-products and generate films with fewer defects. Among different functional groups, styrene,[27–30] acrylate,[31] phenylethynyl group,[32] azide,[33] trifluorovinylether,[34] benzocyclobutene[35] and silane[36] have been widely used as thermally polymerizable functional groups. Specifically, styrene can generate radicals at relatively low temperatures (about 180 °C) and be further polymerized to form a polymer, which provides excellent anti-erosion properties and is suitable for serving as the thermal cross-linking functional group.

In this work, a new electron donor **BCz3Ph** was synthesized and characterized to intermix with a benchmark triazine-based acceptor PO-T2T[37] to form a new exciplex-forming system, which gave a green emission with a decent photoluminescence quantum yield (PLQY) of 43%. For creating a smooth hole
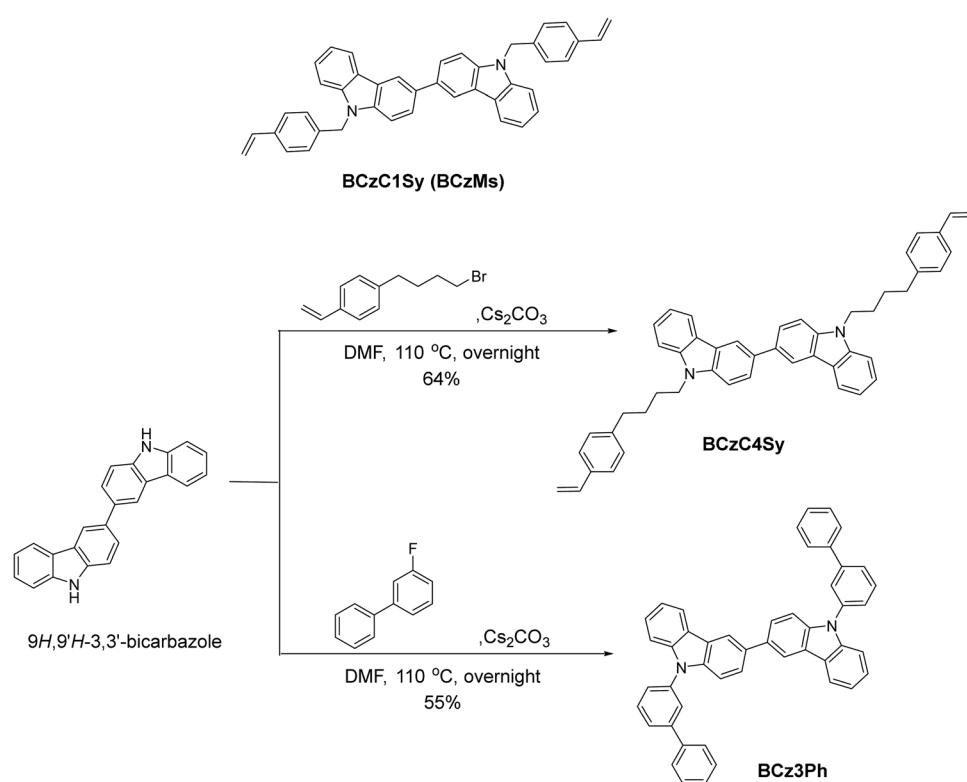
Scheme 1 The structure of model compound **BCzC1Sy** and the syntheses of **BCzC4Sy** and **BCz3Ph**.

This journal is © The Royal Society of Chemistry 2023

J. Mater. Chem. C, 2023, **11**, 1056–1066 | **1057**

injection and transport, dicarbazole was chosen as the core to be further functionalized with a styrene group to afford a new thermally cross-linkable HTM. The choice of dicarbazole as the core of the HTL suppresses the energy barrier between the HTL and EML issue and is also beneficial for preventing the emission color pollution from the exciplex formation at the HTL/EML interface. In a previous study, Lee and coworkers reported a cross-linkable dicarbazole-centered HTM **BCzMs** (**BCzC1Sy**) (Scheme 1),[38] which served as a suitable HTM for solution-processed phosphorescent devices due to its hole-transporting and anti-solvent erosion properties. In this work, the length of the alkyl chain between the dicarbazole core and styrene is increased to afford a new thermally cross-linkable molecule **BCzC4Sy**. The effects of the carbon chain lengths of the hole-transporting materials were found to strongly influence the temperature required for thermal polymerization, in which **BCzC4Sy** exhibits apparent thermal polymerization behavior at a temperature of 146 °C, which is lower than that of 192 °C of **BCzC1Sy**. More importantly, the **BCzC4Sy** film after thermal treatment exhibits excellent solvent erosion resistance. The OLED devices employing thermally cross-linked **BCzC1Sy** and **BCzC4Sy** films as the HTL and the solution-processed **BCz3Ph** : PO-T2T blend as the EML gave EQE_{max} of 7.2% and 9.2%, respectively, while maintaining a high efficiency of 7.1% and 8.9% at 1000 cd m^{-2}. This work highlights the design of a new thermally cross-linkable HTL with the same core chromophore of the donor for exciplex formation. The new molecular monomer **BCzC4Sy** with a more flexible alkyl linkage can thermally polymerize to give a solvent-resistive film with superior properties compared to the **BCzC1Sy** counterpart, affording better performing solution-processed exciplex-based OLED devices with lower efficiency roll-off.

Results and discussion

The molecular structures and synthetic pathways of **BCz3Ph** and **BCzC4Sy** are depicted in Scheme 1. The donor **BCz3Ph** for exploring the exciplex formation was prepared from $9H,9'H$-3,3'-dicarbazole with 3-fluoro-1,1'-biphenyl via S_NAr reaction. **BCzC4Sy** was synthesized from compound $9H,9'H$-3,3'-dicarbazole via S_N2 reaction with 1-(4-bromobutyl)-4-vinylbenzene. All new molecules were characterized with satisfactory spectroscopic data, and the experimental details are provided in the ESI.†

The photophysical behaviors of **BCz3Ph** and **BCzC4Sy** as compared to those of the model counterpart **BCzC1Sy** were investigated by measuring the UV-vis absorption and photoluminescence (PL) spectra, as depicted in Fig. 1a, and the data are summarized in Table 1. In diluted toluene solution at room temperature, similar π–π^* transition absorption peaks were observed for the absorption spectra of **BCzC1Sy** and **BCzC4Sy**, with a maximum absorption peak (λ_{max}) centered around
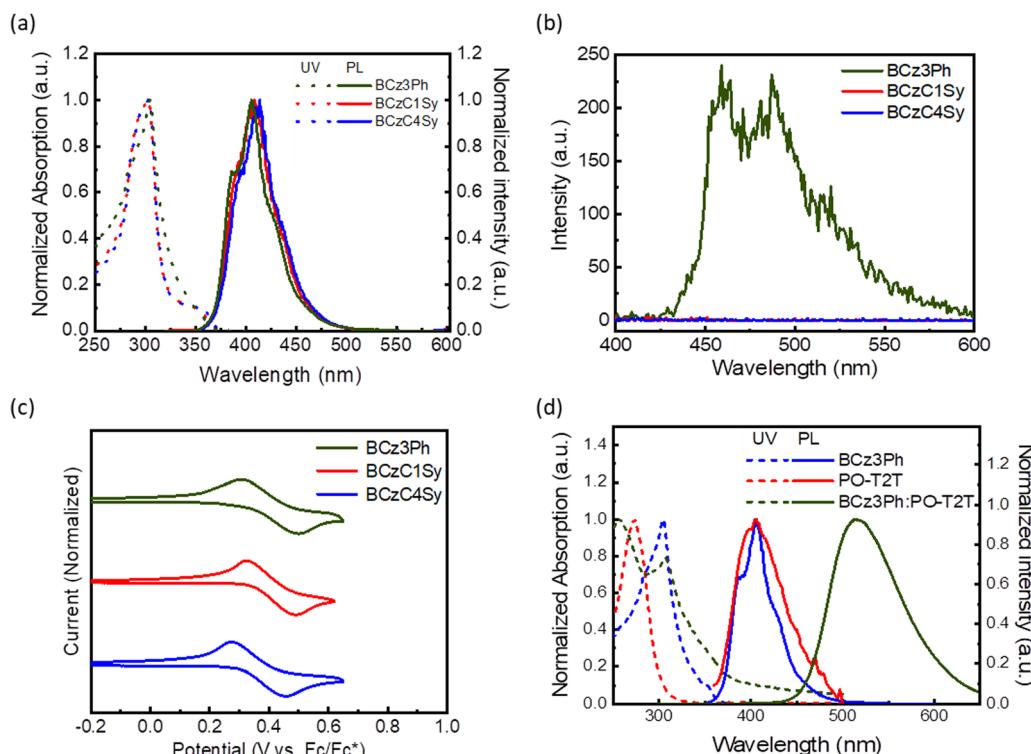

Fig. 1 (a) Absorption and emission spectra of **BCzC1Sy** and **BCzC4Sy** in toluene solution (10^{-5} M). (b) Phosphorescence spectrum of **BCz3Ph**, **BCzC1Sy** and **BCzC4Sy** in MeTHF (10^{-5} M) solution at 77 K. (c) Cyclic voltammograms of **BCz3Ph**, **BCzC1Sy** and **BCzC4Sy**. (d) Absorption and emission spectrum of **BCz3Ph** and PO-T2T films, and **BCz3Ph** : PO-T2T (2 : 1) blended film.

1058 | *J. Mater. Chem. C*, 2023, **11**, 1056–1066

This journal is © The Royal Society of Chemistry 2023

Table 1 Photophysical, electrochemical and thermal properties of **BCz3Ph**, **BCzC1Sy** and **BCzC4Sy**

Molecule	λ_{abs} sol.[a] (nm)	λ_{PL} sol.[a] (nm)	Optical E_g[b] (eV)	E_T[c] (eV)	HOMO[d] (eV)	LUMO[e] (eV)	T_d (°C)	T_{cl} (°C)[g]
BCz3Ph	305	406	3.34	2.90	−5.22[d]	−1.88	454	—
BCzC1Sy	303	409	3.40	—	−5.22[d]	−1.82	430[f]	192
BCzC4Sy	303	414	3.40	—	−5.18[d]	−1.78	453	146

[a] Measured in toluene at the concentration about 10^{-5} M. [b] Optical E_g is calculated from the onset of absorption. [c] Estimated from the onset of the Phos spectra at 77 K in MeTHF. [d] Calculated from potential vs. ferrocene/ferrocenium redox couple. [e] Calculated as the difference between the HOMO and the corresponding optical bandgap. [f] Reported value (ref. 38). [g] T_{cl} is the peak temperature of cross-linking, determined by DSC.

303 nm together with weak absorptions around 330–360 nm corresponding to n–π* transition. It is noted that **BCz3Ph** equipped with an N-biphenyl substituent exhibits similar λ_{max} to those of **BCzC1Sy** and **BCzC4Sy**, but less distinguished n–π* absorption. All three materials show similar emission spectra in toluene solution, and the PL maxima (PL λ_{max}) are centered around 407–414 nm, and are assigned to the dicarbazole core. The phosphorescence spectrum of **BCz3Ph** in MeTHF was then acquired at 77 K, as depicted in Fig. 1b. The T_1 energy level (E_T) can then be estimated to be 2.90 eV from the onset of the phosphorescence spectrum. As a reference, the triplet energy level of **BCzC1Sy** was calculated to be 2.87 eV by density functional theory (DFT) and time-dependent DFT (TD-DFT) under the B3LYP/6-31G level.[40] However, attempts to measure the phosphorescence spectra of **BCzC1Sy** and **BCzC4Sy** were not successful due to the appearance of styrene groups, which are an efficient triplet quencher.[41a–c] The transient photoluminescent (TRPL) spectra of **BCz3Ph** and **BCzC4Sy** shown in Fig. S1 (ESI†) exhibit a much longer lifetime of **BCz3Ph** as compared to that of **BCzC4Sy**, indicating the phosphorescence quenching process in the styrene-appended structure. Furthermore, the absorption and emission of **BCzC1Sy** and **BCzC4Sy** before and after cross-linking were examined as the results shown in Fig. S2 (ESI†). The absorptions remain intact, but the broadening of the emissions was observed after cross-linking, which might have arisen from the aggregation of the chromophore.

Cyclic voltammetry (CV) was then implemented to investigate the electrochemical properties of these materials. The oxidation potential was measured and recorded with reference to the ferrocene/ferrocenium (Fc/Fc⁺) redox couple, as shown in Fig. 1c. A reversible oxidation potential at 0.34, 0.31 and 0.22 V was observed for **BCz3Ph**, **BCzC1Sy** and **BCzC4Sy**, respectively. Apparently, **BCz3Ph** exhibits a higher oxidation potential as compared to those of alkylated counterparts **BCzC1Sy** and **BCzC4Sy** due to the inductive effect of the biphenyl substituents. Also, it is noted that **BCzC1Sy** exhibits a slightly higher oxidation potential as compared to that of **BCzC4Sy** due to the shorter distance of styrene. This result indicates that the length of the alkyl chain has a slight effect on the oxidation behavior. With reference to the Fc/Fc⁺ redox couple, the HOMO energy levels are estimated as 5.22 eV (**BCz3Ph**), 5.22 eV (**BCzC1Sy**),

and 5.18 eV (**BCzC4Sy**). The energy levels of **BCzC1Sy** and **BCzC4Sy** demonstrate that these molecules are suitable for serving as HTMs of OLED devices that employ the exciplex-forming system with **BCz3Ph** as the donor.

According to previous reports, BCzPh has been reported as a superior donor material for exciplex-forming systems when paired with triazine-centered acceptors.[39] Herein, the new donor **BCz3Ph** with an additional phenyl group on the N-substituted peripherals can further enhance the morphological stability. A glass transition temperature (T_g = 140 °C) was identified by differential scanning calorimetry (DSC) as compared to that (60 °C) of BCzPh.[40] In addition, **BCz3Ph** possesses comparable molecular weight with the triazine-based acceptors for better compatibility for film formation upon solution processes. To examine the possibility of forming a suitable exciplex blend, the donor **BCz3Ph** was mixed with a benchmark acceptor PO-T2T. The films were prepared by spin-coating 1.6 wt% solutions of **BCz3Ph**, PO-T2T and a **BCz3Ph**:PO-T2T (2:1) mixture in chlorobenzene to give a thickness of the film of about 30 nm. As shown in Fig. 1d, the absorption spectrum of the **BCz3Ph**:PO-T2T (2:1) blend film can be deemed a linear combination of the individual donor and acceptor absorptions, indicating that no apparent ground state electronic interactions are present. On the other hand, compared with the emissions of **BCz3Ph** and PO-T2T, the emission of the **BCz3Ph**:PO-T2T blend shows a distinctly red-shifted peak centered at 527 nm, which is a signature of exciplex formation in the blend. More importantly, the solution-processed **BCz3Ph**:PO-T2T blend film exhibits a PLQY of 43%, indicating the efficient intermolecular charge transfer between **BCz3Ph** and PO-T2T. The phosphorescence spectrum of the exciplex-forming **BCz3Ph**:PO-T2T (2:1) blend is shown in Fig. S3 (ESI†). The overlapping peaks of the PL and Phos spectra indicate that the singlet state and triplet state of the exciplex are almost degenerate in energy, demonstrating the potential of efficient RISC. To verify the TADF character of the emission from the **BCz3Ph**:PO-T2T (2:1) blend film, temperature-dependent (77–300 K) transient photoluminescence (TRPL) spectra were measured. As indicated in Fig. S4 (ESI†), the relaxation profiles of the **BCz3Ph**:PO-T2T (2:1) film emissions at different temperatures can be fitted with two-component exponential decays. The fitting data at 300 K are summarized in Table 2, while the data of different temperatures are summarized in Table S1 (ESI†). As indicated, the delayed fluorescence ratio of the exciplex-forming blend enhances along with the increase of the temperature, whereas

Table 2 The photophysical characteristics of the **BCz3Ph**:PO-T2T blend films

D:A ratio	PLQY[a] (%)	λ_{PL}/onset (nm)	TRPL[b]			
			A_1	τ_p (ns)	A_2	τ_d (µs)
2:1	43	533/455	0.02	58	0.98	2.59

[a] Measured with an integrating sphere (Hamamatsu C9920-02). [b] Measured under an ambient atmosphere (300 K), and the decay components were fitted with two exponential decay models as $I(t) = A_1 \exp(-t/\tau_p) + A_2 \exp(-t/\tau_d)$, as shown in Fig. S4 (ESI).

This journal is © The Royal Society of Chemistry 2023

J. Mater. Chem. C, 2023, **11**, 1056–1066 | **1059**

the prompt fluorescence ratio slightly decreases as the temperature increases to 300 K. The two-component relaxation as well as the enhanced RISC rates at higher temperatures give rise to an increase in the delayed fluorescence ratio, which is a typical signature of materials with TADF character.

The thermal stability of the carbazole-based materials was investigated with thermogravimetric analysis (TGA) under nitrogen. The TGA analysis indicates that **BCz3Ph** exhibits a higher decomposition temperature ($T_d = 454$ °C, corresponding to 5 wt% loss) as compared to that (430 °C) of BCzPh.[40] **BCzC4Sy** exhibits good thermal stability with a T_d of 453 °C, which is higher than that (430 °C)[38] of **BCzC1Sy**, mainly attributed to its larger molecular weight. In addition, the feasible preparation of the D:A blended film reveals its suitability to serve as the EML of a solution-processed OLED device. For smooth hole injection to the EML, a solvent-resistant HTL is highly desired. To probe the thermal cross-linking temperatures of **BCzC1Sy** and **BCzC4Sy**, the materials were investigated by DSC at a heating rate of 10 °C min^{-1}, and the results are shown in Fig. 2a. The cross-linkable materials **BCzC1Sy** and **BCzC4Sy** showed significant exothermic peaks at 192 °C and 142 °C, respectively, indicating that the cross-linking reactions occurred around these temperatures. The DSC profiles show a large difference between these two molecules. The exothermic peak of **BCzC1Sy** is about 50 °C higher as compared to that of **BCzC4Sy**. Apparently, the longer butyl (C4) chain of **BCzC4Sy**

increases the flexibility and reactivity of the cross-linking styrene group, in turn facilitating the cross-linking reaction at a lower temperature.

In order to confirm the solvent resistance of these two thermally cross-linkable materials, an experiment was conducted to examine the solvent erosion effects *via* monitoring the difference in the absorption intensity of the thermally cross-linked films before and after the solvent treatment. Initially, the absorption intensities of the **BCzC1Sy** and **BCzC4Sy** films that have been thermally treated at 100 and 170 °C for thermal cross-linking and subsequently treated with chlorobenzene that was dripped onto the films and dried by spin-coating were measured. For comparison, the non-cross linkable **BCz3Ph** was also used as a model compound for examining the solvent resistance. As the spectra indicated in Fig. 2b, chlorobenzene erodes most of the **BCz3Ph** molecules, causing the intensity of its absorption to be significantly reduced. In contrast, the **BCzC1Sy** films have improved solvent resistance after thermal treatment at 100 and 170 °C as compared to that of the **BCz3Ph** film (Fig. 2c), despite displaying little temperature dependence. With the aid of the flexible C4 alkyl chain, the **BCzC4Sy** film after thermal cross-linking at 170 °C has a significant degree of resistance to solvent erosion as the absorption remains nearly unchanged under solvent washing (Fig. 2d). This result indicates that **BCzC4Sy** has perfect solvent erosion resistant after thermal cross-linking and can serve as a good HTL for
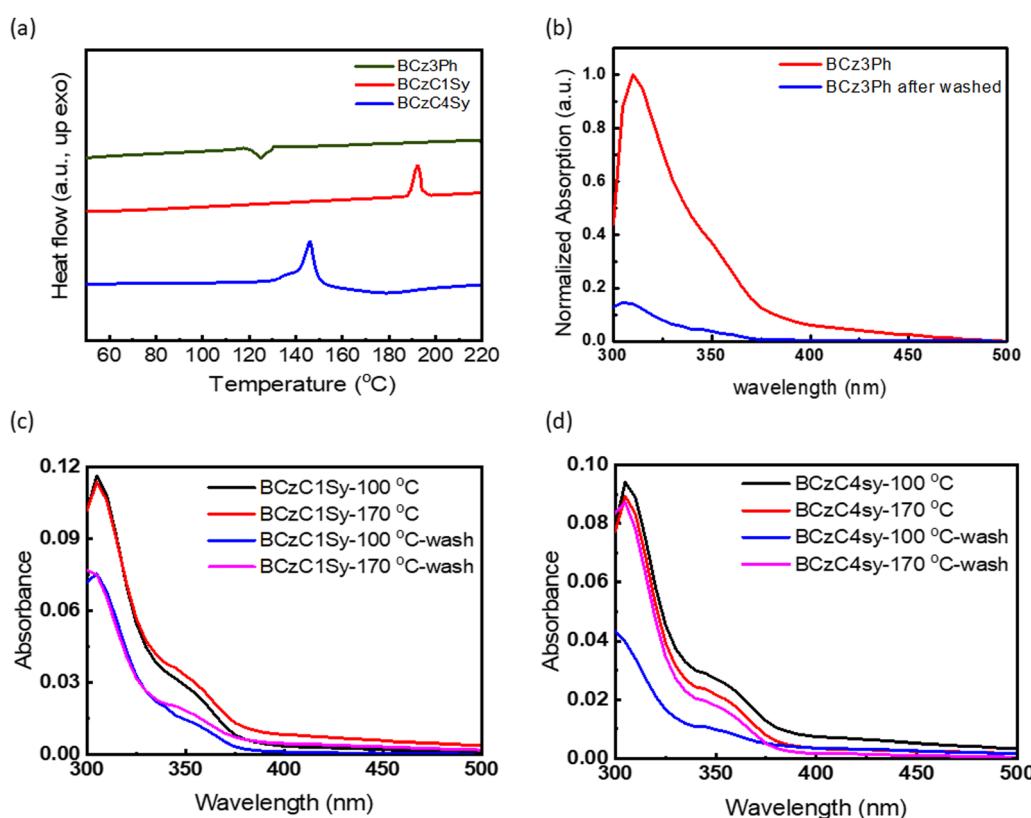
Fig. 2 (a) DSC thermogram of **BCz3Ph**, **BCzC1Sy** and **BCzC4Sy**. (b) Absorption spectra of the **BCz3Ph** film before and after chlorobenzene washing; absorption spectra of the (c) **BCzC1Sy**, and (d) **BCzC4Sy** film treated at 100 °C before (black line) and after being washed (blue line) with chlorobenzene, and heated to 170 °C before (red line) and after being washed (magenta line) with chlorobenzene.

1060 | *J. Mater. Chem. C*, 2023, **11**, 1056–1066

This journal is © The Royal Society of Chemistry 2023
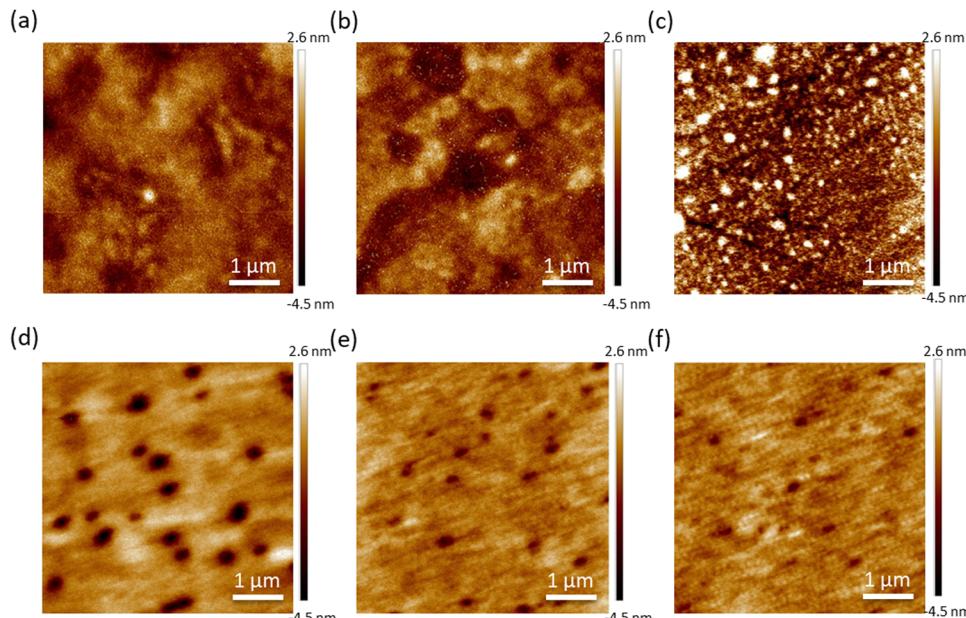
Fig. 3 AFM images of cross-linkable hole transporting materials. All substrates were baked at 100 °C for 10 min to remove residual solvent. (a) **BCzC1Sy** before thermal annealing. (b) **BCzC1Sy** annealed at 170 °C for 30 min. (c) **BCzC1Sy** after being washed by chlorobenzene. (d) **BCzC4Sy** before thermal annealing. (e) **BCzC4Sy** annealed at 170 °C for 30 min. (f) **BCzC4Sy** after being washed by chlorobenzene. The root mean square roughness is (a) 0.68 nm, (b) 0.80 nm, (c) 1.39 nm, (d) 0.83 nm, (e) 0.56 nm, and (f) 0.52 nm.

solution-processed OLED devices. Furthermore, **BCzC4Sy** can be washed away prior to thermal cross-linking, which means that it has a great operating window and is thus more versatile in the fabrication of OLED devices.

Atomic force microscopy (AFM) was further used to examine the integrity of the film morphology and provide insight towards the better solvent resistance of **BCzC4Sy**. Here, the films were measured before and after thermal cross-linking, along with rinsing with chlorobenzene, respectively. The results are shown in Fig. 3. The root mean square (RMS) value (0.68 nm) of **BCzC1Sy** shows that the film is quite smooth at the beginning, but it then slightly increases to 0.80 nm after thermal cross-linking. After rinsing with chlorobenzene, the RMS value was further deteriorated to 1.39 nm, which means that the film coating by the polymerized **BCzC1Sy** can't resist solvent erosion very well. On the other hand, the RMS value (0.83 nm) of **BCzC4Sy** is larger than that of **BCzC1Sy** before thermal cross-linking, indicating that the surfaces of the films were relatively rough. By thermal cross-linking of **BCzC4Sy**, the RMS value was found to reduce to 0.56 nm. After further rinsing with chlorobenzene, the RMS value can still be maintained at 0.52 nm, demonstrating that the polymerized **BCzC4Sy** can indeed effectively resist solvent erosion after thermal cross-linking, and the surface morphology of the films can still be retained after solvent rinsing.

Device

To evaluate the potential of the cross-linkable materials as the HTLs for solution-processed OLEDs, devices were fabricated with the architecture configured as: ITO/PEDOT:PSS (40 nm)/**BCzCnSy** (*n* = 1 or 4; 40 nm)/**BCz3Ph**:PO-T2T (in ratio 2:1,

40 nm)/CN-T2T (60 nm)/LiF/Al. The device structure is shown in Fig. 4a. The **BCzCnSy** (*n* = 1 or 4) molecules possess a compatible HOMO energy level to the EML and high triplet energy, making them suitable for acting as the HTLs. CN-T2T was selected as the electron transporting layer (ETL) owing to its high triplet energy level (E_T = 2.82 eV), high thermal stability (T_d > 400 °C) and high electron mobility ($\mu_e \sim 10^{-4}$ cm^2 V^{-1} s^{-1} order).[42] It is also crucial that the LUMO of CN-T2T is slightly higher than that of PO-T2T, such that the electron injection process across the interface is much more efficient.[37] Fig. 4b shows the energy levels of the HTMs, **BCz3Ph**, PO-T2T, and CN-T2T.

First, the thermally cross-linked (170 °C) **BCzC1Sy** film was utilized for screening the suitable D:A ratio for giving the best EML. After examining the device characteristics (Fig. S5 and Table S2, ESI†), **BCz3Ph**:PO-T2T = 2:1 (PLQY = 43%) was selected as the EML owing to its pure exciplex emission. Therefore, four devices (the combination of two HTLs and two curing temperatures) were fabricated. All devices show green EL emission with wavelength peaks between 531 and 535 nm and the CIE coordinate of approximately (0.36, 0.55). The device characteristics are summarized in Table 3. Fig. 5a shows the current density–voltage–luminance (*J–V–L*) characteristics of the devices. The D1 and D2 devices employing **BCzC1Sy** and **BCzC4Sy** films annealed at 100 °C as the HTLs exhibit the same V_{on} of 3.3 V, whereas the V_{on} of the D3 and D4 devices employing the **BCzC1Sy** and **BCzC4Sy** films annealed at 170 °C as the HTLs are 2.7 and 2.5 V, respectively. The V_{on} is drastically reduced when the annealing temperature is raised to 170 °C, which is attributed to the more sufficient cross-linking polymerization at a higher temperature, resulting in a

This journal is © The Royal Society of Chemistry 2023

J. Mater. Chem. C, 2023, **11**, 1056–1066 | **1061**
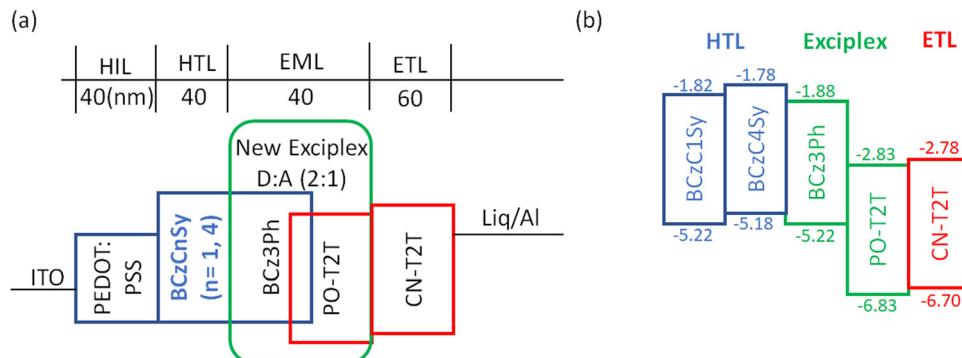
Fig. 4 (a) Schematic OLED structure, and (b) energy levels of the HTLs, donor, acceptor and ETL used in this study.

Table 3 Summary of the optimized OLED performance

Device	HTL	Annealing Temp. (°C)	EL λ_{max} (nm)	$V_{on}{}^{a}$ (V)	EQE$_{max}$/CE$_{max}$/PE$_{max}$ (%/cd A^{-1}/lm W^{-1})	At 1000 cd m^{-2} (%/cd A^{-1}/lm W^{-1})^{b}	L_{max} (cd m^{-2})	CIE (x, y)
D1	BCzC1Sy	100	531	3.3	5.53/17.24/11.22	5.46/16.75/11.21	22 904	(0.36, 0.55)
D2	BCzC4Sy	100	533	3.3	6.25/19.33/13.18	6.21/19.14/13.07	22 222	(0.36, 0.55)
D3	BCzC1Sy	170	531	2.7	7.15/21.82/18.68	7.07/21.26/15.90	23 287	(0.37, 0.55)
D4	BCzC4Sy	170	531	2.5	9.21/27.94/28.7	8.89/26.87/21.65	22 137	(0.37, 0.55)

^{a} Turn-on voltage at which emission became detectable. ^{b} The values of EQE, CE, PE and driving voltages of the device at 1000 cd m^{-2}.

smoother film morphology for better hole injection and transport. As indicated in Fig. 5b–d, the devices utilizing these cross-linkable materials as HTLs demonstrate decent EQEs of over 5%. More importantly, after thermal cross-linking at 170 °C, the EQEs of the devices are significantly increased to 7.2% and 9.2% for devices D3 and D4, respectively. It is noteworthy that the EQEs of the D3 and D4 devices remain at 7.1% and 8.9% at 1000 cd m^{-2}, respectively, indicating the reduced efficiency roll-off and device stability. Furthermore, the D4 device exhibited the lowest V_{on} and excellent efficiencies of 9.2% (EQE), 27.94 cd A^{-1} (CE) and 28.7 lm W^{-1} (PE), which is the best performance among the reported solution-processed exciplex-based OLEDs. Generally, $\eta_{EQE} = \eta_{out} \times \beta \times \gamma \times \Phi_{PL}$,[43] where β is the exciton generation factor induced from photons, γ is the carrier balance factor of the ratio between holes and electrons, and Φ_{PL} is the PLQY. Given that the PLQY of the exciplex is 43%, η_{out} is assumed to be 20%, and the theoretical EQE can be deduced to be 9.8%, which is very close to that of the D4 device. This indicates that the D4 device based on thermally cross-linked **BCzC4Sy** film is well optimized to extract the maximum efficiency of the EML. The film integrity of the **BCzC4Sy** film achieved by the thermal cross-linking process is speculated to lead to the high EQE of the device. It has been reported that the cross-linked molecules would achieve the most thermodynamically stable molecular arrangement through slight writhing after film formation.[44] Due to the longer side chain of **BCzC4Sy**, it is endowed with the highest degree of freedom to attain the most stable and complete polymer film, leading to superior solvent resistance and better hole-transporting capability under the same thermal curing conditions. This is the reason why the D4 device achieves the highest EQE, CE, PE and lower V_{on}.

To avoid HTLs forming an exciplex with PO-T2T for giving different emission color at the HTL/EML interface, dicarbazole was selected as the core of the HTM and the donor of the exciplex. In order to verify this idea, bilayer-type films were made with the PO-T2T coating on top of the bare **BCzC4Sy** film or thermally cross-linked **BCzC4Sy** film. The photoluminescence spectra of these bilayer films are shown in Fig. S6 (ESI†) as compared to that of the film fabricated with the exciplex-forming blend **BCz3Ph** : PO-T2T. Despite its weaker emission intensity, **BCzC4Sy** can indeed form the same exciplex emission as **BCz3Ph** with PO-T2T, confirming that the common dicarbazole core of **BCz3Ph** and **BCzC4Sy** is crucial to circumvent the pollution of the desired exciplex emission from unwanted interfacial interactions.

In addition, it is of great significance to demonstrate a large-area device fabricated under ambient environments, as it is beneficial to practical mass production and potential lighting applications. Slot-die coating is considered to be a well-suited means of achieving extremely uniform large area films among various solution-process technologies, due to the simple relationship between the flow rate of the solution, wet-film coating thickness, and speed of the coated substrate relative to the head. Besides, slot-die coating can be easily integrated into scaled-up processes, including sheet-to-sheet deposition and roll-to-roll coating systems. While the desired thickness of the film is on the scale of nanometers, the thickness of the as-coated wet film is on the scale of micrometers,[45] containing mass solvent residues. It is thus crucial that the under layer, in this case the HTM, presents superior solvent resistance. Herein, a large-area 2 × 2 cm^{2} device (device D5) adopting the device structure of D4 with the thermally cross-linked **BCzC4Sy** film as

1062 | *J. Mater. Chem. C*, 2023, **11**, 1056–1066

This journal is © The Royal Society of Chemistry 2023
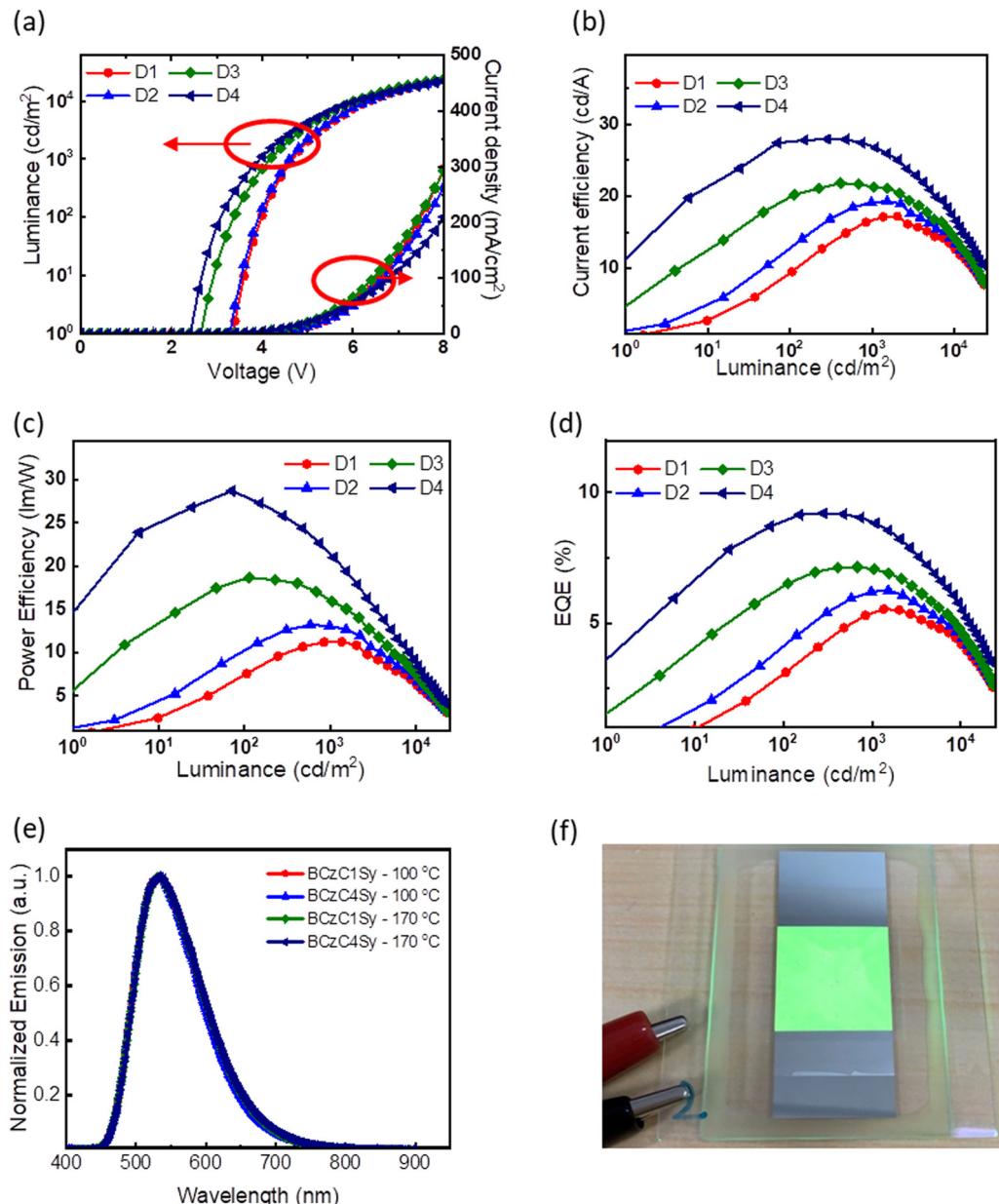
Fig. 5 (a) Luminance–voltage–current density characteristics, (b) current efficiency–luminance characteristics, (c) power efficiency-luminance characteristics, (d) EQE-luminance characteristics and (e) normalized EL spectra for the devices employing **BCzC1Sy** and **BCzC4Sy** as HTLs, with or without thermal cross-linking, and (f) the photograph of device D5 prepared with the slot-die method.

the HTL was prepared in ambient atmosphere employing the slot-die coating technique, as shown in Fig. 5f. The flow rates and concentrations of solution, and the speeds of the coated head for each layer are listed in Table S3 (ESI†). The results of device D5 are shown in Fig. S7 and Table S4 (ESI†). The EQEs and L_{max} remain at 5.0% and 20686 cd m^{-2}, respectively, which demonstrates high stability of the solution-processed **BCzC4Sy** film as the HTL and **BCz3Ph**:PO-T2T blended system as the EML in air. The bright and uniform green emission (Fig. 5f) without visible pinholes confirms the high solvent and air resistance of the thermally cross-linked **BCzC4Sy** film. It is noteworthy that the solvent resistance is a major limit of the

slot-die coating method, it is evident that with the incorporation of a thermally cross-linkable material **BCzC4Sy**, a large-area OLED device with good efficiencies can be accomplished without using expensive vacuum deposition and extra operations with intricate exclusion of humidity and oxygen.

Conclusion

A new green exciplex-forming system comprising a **BCz3Ph**:POT2T (2:1) blend with PL λ_{max} of 527 nm and a high PLQY of 43% was identified to show TADF properties and exploited as

This journal is © The Royal Society of Chemistry 2023

J. Mater. Chem. C, 2023, **11**, 1056–1066 | **1063**

the emitting layer of solution-processed OLEDs. Simultaneously, a new thermal cross-linkable hole-transporting monomer **BCzC4Sy** bearing a dicarbazole core with two butyl chain-linked styrenes was designed and synthesized. As compared to the reported model monomer **BCzC1Sy**, the effects of the linker length between styrene and dicarbazole on the thermal curing behavior and physical properties of the molecules and thermally polymerized films are examined. **BCzC4Sy** was found to undergo thermal polymerization at a lower temperature (142 °C) than that (192 °C) of **BCzC1Sy** due to the more flexible C4-linker. The absorptions of these thermally treated HTM films at different temperatures before and after chlorobenzene rinsing indicate that the thermally polymerized **BCzC4Sy** film can exhibit better solvent resistance. In addition, the AFM analyses found that the RMS difference of the **BCzC4Sy** film upon chlorobenzene rinsing was limited, indicating that the film had high integrity. Among the OLED devices with thermally cross-linked **BCzC1Sy** and **BCzC4Sy** films as HTLs, device D4 employing the **BCzC4Sy** film as the HTL and **BCz3Ph** : POT2T (2 : 1) blend as the EML gave the best EQE_{max} of 9.2%, $CE_{max} = 27.94$ cd A^{-1} and $PE_{max} = 28.7$ lm W^{-1}, and a maximum luminance of over 22 000 cd m^{-2}. This device also exhibited a low efficiency roll-off, retaining 97% of the maximum EQE at 1000 cd A^{-1}. Our results demonstrate the successful use of thermal cross-linkable materials to achieve a good solvent resistant HTL with a compatible HOMO energy level to the EML for hole injection and suppressing the complexity of possible exciplex emission from the HTL/EML interface. More significantly, a 2 × 2 cm^2 device adopting the D4 device configuration fabricated by the slot-die coating technique was realized with rather good device efficiency, which provides vast potential in the large-scale fabrication of solution-processed OLED devices for lighting applications in the future.

Conflicts of interest

There are no conflicts of interest to declare.

Acknowledgements

References

1 B. Geffroy, P. I. Roy and C. Prat, Organic Light-Emitting Diode (OLED) Technology: Materials, Devices and Display Technologies, *Polym. Int.*, 2006, **55**, 572–582.

2 S. R. Forrest, The path to ubiquitous and low-cost organic electronic appliances on plastic, *Nature*, 2004, **428**, 911–918.

3 M. Ikai and S. Tokito, Highly efficient phosphorescence from organic light-emitting devices with an exciton-block layer, *Appl. Phys. Lett.*, 2001, **79**, 156–158.

4 H. Kaji, H. Suzuki, T. Fukushima, K. Shizu, K. Suzuki, S. Kubo, T. Komino, H. Oiwa, F. Suzuki, A. Wakamiya, Y. Murata and C. Adachi, Purely organic electroluminescent material realizing 100% conversion from electricity to light, *Nat. Commun.*, 2015, **6**, 8476.

5 K.-H. Kim and J.-J. Kim, Origin and Control of Orientation of Phosphorescent and TADF Dyes for High-Efficiency OLEDs, *Adv. Mater.*, 2018, **30**, 1705600.

6 A. Endo, K. Sato, K. Yoshimura, T. Kai, A. Kawada, H. Miyazaki and C. Adachi, Efficient up-conversion of triplet excitons into a singlet state and its application for organic light emitting diodes, *Appl. Phys. Lett.*, 2011, **98**, 083302.

7 K. Kawasumi, T. Wu, T. Zhu, H. S. Chae, T. V. Voorhis, M. A. Baldo and T. M. Swager, Thermally activated delayed fluorescence materials based on homoconjugation effect of donor–acceptor triptycenes, *J. Am. Chem. Soc.*, 2015, **137**, 11908–11911.

8 T.-L. Wu, M.-J. Huang, C.-C. Lin, P.-Y. Huang, T.-Y. Chou, R.-W. Cheng, H.-W. Lin, R.-S. Liu and C.-H. Cheng, Diboron compound-based organic light-emitting diodes with high efficiency and reduced efficiency roll-off, *Nat. Photonics*, 2018, **12**, 235–240.

9 W. Zeng, H.-Y. Lai, W.-K. Lee, M. Jiao, Y.-J. Shiu, C. Zhong, S. Gong, T. Zhou, G. Xie, M. Sarma, K.-T. Wong, C.-C. Wu and C. Yang, External quantum efficiency for orange–red organic light emitting diodes by employing thermally activated delayed fluorescence emitters composed of 1,8-naphthalimideacridine hybrids, *Adv. Mater.*, 2018, **30**, 1704961.

10 (*a*) X.-K. Liu, Z. Chen, C.-J. Zheng, M. Chen, W. Liu, X.-H. Zhang and C.-S. Lee, Nearly 100% triplet harvesting in conventional fluorescent dopant-based organic light-emitting devices through energy transfer from exciplex, *Adv. Mater.*, 2015, **27**, 2025–2030; (*b*) M. Zhang, C.-J. Zheng, H. Lin and S.-L. Tao, Thermally activated delayed fluorescence exciplexemitters for high-performance organiclight-emitting diodes, *Mater. Horiz.*, 2021, **8**, 401; (*c*) J. Guo, Y. Zhen, H. Dong and W. Hu, Recent progress on organic exciplex materialswith different donor–acceptor contacting modesfor luminescent applications, *J. Mater. Chem. C*, 2021, **9**, 16843–16858; (*d*) M. Sarma and K.-T. Wong, Exciplex: An Intermolecular Charge-Transfer Approach for TADF, *ACS Appl. Mater. Interfaces*, 2018, **10**(23), 19279–19304; (*e*) M. Sarma, L.-M. Chen, Y.-S. Chen and K.-T. Wong, Exciplexes in OLEDs: Principles and promises, *Mater. Sci. Eng., R*, 2022, **150**, 1006.

11 M. Zhang, C.-J. Zheng, H. Lin and S.-L. Tao, Thermally activated delayed fluorescence exciplex emitters for highperformance organic light-emitting diodes, *Mater. Horiz.*, 2021, **8**, 401–425.

12 M. Zhang, C.-J. Zheng, K. Wang, Y.-Z. Shi, D.-Q. Wang, X. Li, H. Lin, S.-L. Tao and X.-H. Zhang, Hydrogen-Bond-Assisted Exciplex Emitters Realizing Improved Efficiencies and Stabilities in Organic Light Emitting Diodes, *Adv. Funct. Mater.*, 2021, **31**, 2010100.

13 K. Goushi and C. Adachi, Efficient organic light-emitting diodes through up-conversion from triplet to singlet excited states of exciplexes, *Appl. Phys. Lett.*, 2012, **101**, 023306.

1064 | *J. Mater. Chem. C*, 2023, **11**, 1056–1066

This journal is © The Royal Society of Chemistry 2023

14 Y.-C. Hu, Z.-L. Lin, T.-C. Huang, J.-W. Lee, W.-C. Wei, T.-Y. Ko, C.-Y. Lo, D.-G. Chen, P.-T. Chou, W.-Y. Hung and K.-T. Wong, New exciplex systems composed of triazatruxene donors and N-heteroarene-cored acceptors, *Mater. Chem. Front.*, 2020, **4**, 2029–2039.

15 L.-M. Chen, I.-H. Lin, Y.-C. You, W.-C. Wei, M.-J. Tsai, W.-Y. Hung and K.-T. Wong, Substitution effect on carbazole-centered donors for tuning exciplex systems as cohost for highly efficient yellow and red OLEDs, *Mater. Chem. Front.*, 2021, **5**, 5044–5054.

16 V. Jankus, C.-J. Chiang, F. Dias and A. P. Monkman, Deep blue exciplex organic light-emitting diodes with enhanced efficiency; p-type or e-type triplet conversion to singlet excitons?, *Adv. Mater.*, 2013, **25**, 1455–1459.

17 Y. J. Cho, S. Taylor and H. Aziz, Increased Electromer Formation and Charge Trapping in Solution- Processed versus Vacuum-Deposited Small Molecule Host Materials of Organic Light-Emitting Devices, *ACS Appl. Mater. Interfaces*, 2017, **9**, 40564–40572.

18 Z.-L. Tseng, W.-L. Huang, T.-H. Yeh, Y.-X. Xu and C.-H. Chiang, Thermally Activated Delayed Fluorescence in CommerciallyAvailable Materials for Solution-Process Exciplex OLEDs, *Polymers*, 2021, **13**, 1668.

19 K. Tong, X. Liu, F. Zhao, D. Chen and Q. Pei, Efficient Light Extraction of Organic Light-Emitting Diodes on a Fully Solution-Processed Flexible Substrate, *Adv. Opt. Mater.*, 2017, **5**, 1700307.

20 T. Chiba, Y.-J. Pu and J. Kido, Solution-Processed White Phosphorescent Tandem Organic Light-Emitting Devices, *Adv. Mater.*, 2015, **27**, 4681–4687.

21 Q. Huang, G. Evmenenko, P. Dutta and T. J. Marks, Molecularly ''Engineered'' Anode Adsorbates for Probing OLED Interfacial Structure-Charge Injection/Luminance Relationships: Large, Structure-Dependent Effects, *J. Am. Chem. Soc.*, 2003, **125**, 14704–14705.

22 W. Hua, Z. Liu, L. Duan, G. Dong, Y. Qiu, B. Zhang, D. Cui, X. Tao, N. Cheng and Y. Liu, Deep-blue electroluminescence from nondopedand doped organic light-emitting diodes (OLEDs)based on a new monoaza[6]helicene, *RSC Adv.*, 2015, **5**, 75–84.

23 M. Zhao, H. Zhang, C. Gu and Y. Ma, Electrochemical polymerization: an emergingapproach for fabricating high-quality luminescentfilms and super-resolution OLEDs, *J. Mater. Chem. C*, 2020, **8**, 5310.

24 C. Liu, H. Luo, G. Shi, J. Yang, Z. Chic and Y. Ma, Luminescent network film depositedelectrochemically from a carbazole functionalizedAIE molecule and its application for OLEDs, *J. Mater. Chem. C*, 2015, **3**, 3752.

25 N. Aizawa, Y.-J. Pu, T. Chiba, S. Kawata, H. Sasabe and J. Kido, Instant Low-Temperature Cross-Linking of Poly(*N*-vinylcarbazole) for Solution-Processed Multilayer Blue Phosphorescent Organic Light-Emitting Devices, *Adv. Mater.*, 2014, **26**, 7543–7546.

26 J. Wang, H. Liu, S. Wu, Y. Jia, H. Yu, X. Li and S. Wang, Chemically doped hole transporting materials with low cross-linking temperature and high mobility for solution-processed green/red PHOLEDs, *Chem. Eng. J.*, 2020, **391**, 12347.

27 W. Jiang, X. Ban, M. Ye, Y. Sun, L. Duan and Y. Qiu, A high triplet energy small molecule based thermally cross-linkable hole-transporting material for solution-processed multilayer blue electrophosphorescent devices, *J. Mater. Chem. C*, 2015, **3**, 243.

28 N. Aizawa, Y.-J. Pu, H. Sasabe and J. Kido, Thermally cross-linkable host materials for enabling solution-processed multilayer stacks in organic light-emitting devices, *Org. Electron.*, 2013, **14**, 1614.

29 W.-Y. Hung, C.-Y. Lin, T.-L. Cheng, S.-W. Yang, A. Chaskar, G.-L. Fan, K.-T. Wong, T.-C. Chao and M.-R. Tseng, A new thermally crosslinkable hole injection material for OLEDs, *Org. Electron.*, 2012, **13**, 2508.

30 J.-H. Jou, T.-H. Li, S. Kumar, C.-C. An, A. Agrawal, S.-Z. Chen, P.-H. Fang, G. Krucaite, S. Grigalevicius, J. Grazulevicius and C.-F. Sung, Enabling high-efficiency organic light-emitting diodes with a cross-linkable electron confining hole transporting material, *Org. Electron.*, 2015, **24**, 254.

31 N. Du, R. Tian, J. Peng, Q. Mei and M. Lu, Cross-linked alq3-containing polymers with improved electroluminescence efficiency used for OLEDs, *Macromol. Rapid Commun.*, 2006, **27**, 412–417.

32 B. G. Kang, H. Kang, N. G. Kang, C. L. Lee, K. Lee and J.-S. Lee, Thermally crosslinkable hole transporting polymer synthesized by living anionic polymerization for effective electron blocking and reduction of exciton quenching in multilayer polymer light emitting diodes, *Polym. Chem.*, 2013, **4**, 969–977.

33 R. Pötzsch and B. Voit, Thermal and photochemical crosslinking of hyperbranched polyphenylene with organic azides, *Macromol. Rapid Commun.*, 2012, **33**, 635–639.

34 Y. H. Niu, M. S. Liu, J. W. Ka and A. K. Y. Jen, Thermally crosslinked hole-transporting layers for cascade hole-injection and effective electron-blocking/exciton-confinement in phosphorescent polymer light-emitting diodes, *Appl. Phys. Lett.*, 2006, **88**, 93505.

35 B. Ma, F. Lauterwasser, L. Deng, C. S. Zonte, B. J. Kim, J. M. J. Fréchet, C. Borek and M. E. Thompson, New thermally cross-linkable polymer and its application as a holetransporting layer for solution processed multilayer organic light emitting diodes, *Chem. Mater.*, 2007, **19**, 4827–4832.

36 S. Lee, Y.-Y. Lyu and S.-H. Lee, The use of cross-linkable interlayers to improve device performances in blue polymer light-emitting diodes, *Synth. Met.*, 2006, **156**, 1004–1009.

37 M. Sarma and K.-T. Wong, Exciplex: An Intermolecular Charge-Transfer Approach for TADF, *ACS Appl. Mater. Interfaces*, 2018, **10**, 19279–19304.

38 S. Ameen, J. Lee, H. Han, M. C. Suh and C. Lee, Curing temperature reduction and performance improvement of solution-processable holetransporting materials for phosphorescent OLEDs by manipulation of cross-linking functionalities and core structures, *RSC Adv.*, 2016, **6**, 33212–33220.

39 M. Wang, Y.-H. Huang, K.-S. Lin, T.-H. Yeh, J. Duan, T.-Y. Ko, S.-W. Liu, K.-T. Wong and B. Hu, Revealing the

This journal is © The Royal Society of Chemistry 2023

J. Mater. Chem. C, 2023, **11**, 1056–1066 | **1065**

Cooperative Relationship between Spin, Energy, and Polarization Parameters toward Developing High-Efficiency Exciplex Light-Emitting Diodes, *Adv. Mater.*, 2019, **31**, 1904114.

40 H. Sasabe, N. Toyota, H. Nakanishi, T. Ishizaka, Y.-J. Pu and J. Kido, 3,3′-Bicarbazole-Based Host Materials for High-Efficiency Blue Phosphorescent OLEDs with Extremely Low Driving Voltage, *Adv. Mater.*, 2012, **24**, 3212–3217.

41 (*a*) R. E. Rebbert and P. Ausloos, Quenching of the Triplet State of Acetone and Biacetyl by various Unsaturated Hydrocarbons, *J. Am. Chem. Soc.*, 1965, **87**, 24; (*b*) R. Bonneau and B. Herran, Structure and Properties of the Triplet State of Styrene Derivatives Studied by Laser-Flash-Photolysis, *Laser Chem.*, 1984, **4**, 151–170; (*c*) D. Koyama and A. J. Orr-Ewing, Triplet State formation and quenching dynamics of 2-mercaptobenzothiazole in solution, *Phys. Chem. Chem. Phys.*, 2016, **18**, 26224.

42 D. K. Dubey, S. S. Swayamprabha, R. A. K. Yadav, D. Tavgenieneb, D. Volyniuk, S. Grigalevicius and J.-H. Joua, A thermally cross-linkable hole-transporting small-molecule for efficient solution-processed organic light emitting diodes, *Org. Electron.*, 2019, **73**, 94–101.

43 T. Miwa, S. Kubo, K. Shizu, T. Komino, C. Adachi and H. Kaji, Blue organic light-emitting diodes realizing external quantum efficiency over 25% using thermally activated delayed fluorescence emitters, *Sci. Rep.*, 2017, **7**, 284.

44 Y. Wada, H. Nakagawa, S. Matsumoto, Y. Wakisaka and H. Kaji, Organic light emitters exhibiting very fast reverse intersystem crossing, *Nat. Photonics*, 2020, **14**, 643–664.

45 M. Schmitt, P. Scharfer and W. Schabel, Slot die coating of lithium-ion battery electrodes: investigationson edge effect issues for stripe and pattern coatings, *J. Coat. Technol. Res.*, 2014, **11**, 57–63.